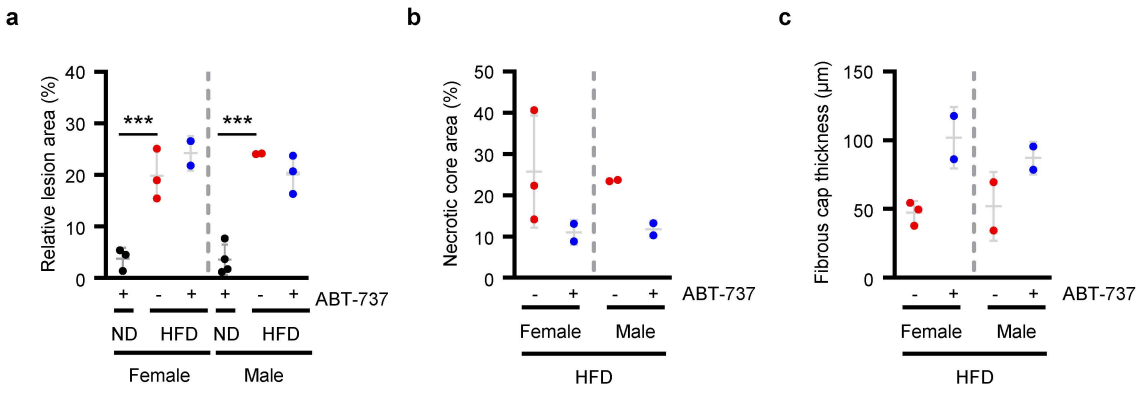

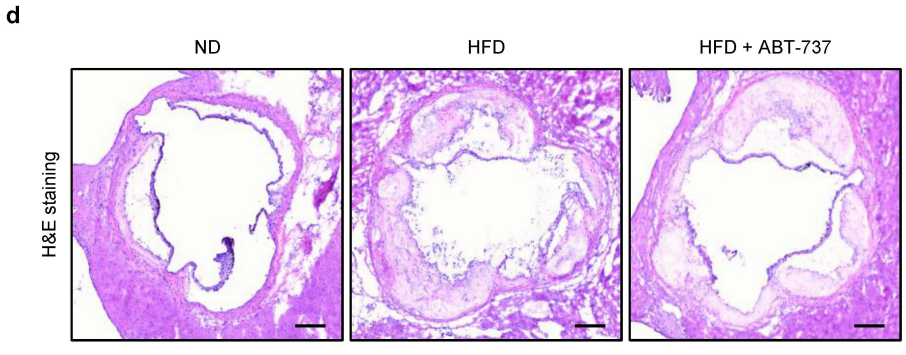

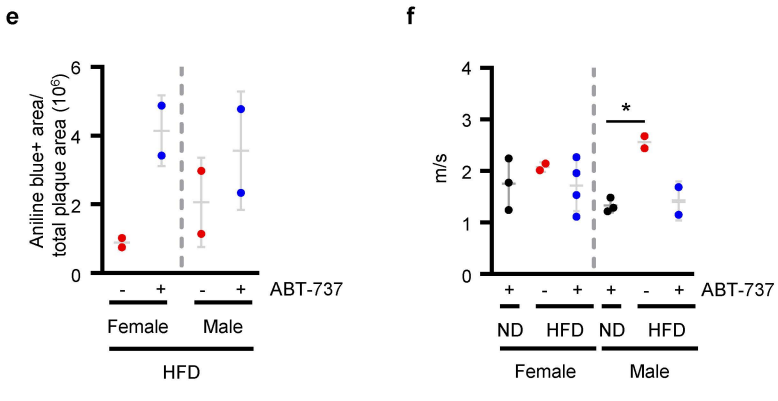

g

Quality control

	Female ND	Female HFD	Female HFD + ABT-737	Male ND	Male HFD	Male HFD + ABT-737
Estimated Number of Cells	5,469	2,635	6,084	5,775	4,988	4,888
Fraction Reads in Cells	82.3%	75.2%	85.5%	74.6%	81.0%	84.6%
Mean Reads per Cell	54,698	58,897	58,233	55,336	69,127	58,106
Median UMI Counts per Cell	6,026	6,817	8,659	5,965	9,040	7,196
Median Genes per Cell	2,229	2,280	2,313	2,210	2,816	2,430
Total Genes Detected	24,060	22,715	24,439	24,072	24,260	23,919

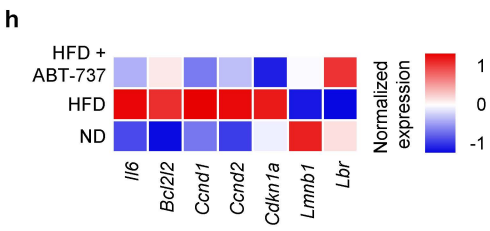

Supplemental Fig. 1 | Atherosclerotic plaque pathology analysis and quality control analysis. a, Quantification of plaque size presented by sex and condition (ND, HFD, and HFD + ABT-737). **b,** Quantification of necrotic core area presented by sex and condition (ND, HFD, and HFD + ABT-737). **c,** Quantification by plaque fibrous cap thickness presented by sex and condition (ND, HFD, and HFD + ABT-737). **d,** Representative H&E staining of aortic roots from ND, HFD, and HFD + ABT-737. The scale bar is 200 µm**. e,** Quantification of collagen fibers (Aniline blue) area / area of aortic root presented by sex and condition (ND, HFD, and HFD + ABT-737). **f,** Pulse wave velocity (PWV) measurements presented by sex and condition (ND, HFD, and HFD + ABT-737). **g,** Quality control table of the scRNA-seq samples including estimated number of cells, fraction reads in cells, mean reads per cell, median UMI counts per cell, median genes per cell, and total genes detected. **h,** Heatmap of normalized expression levels of classical senescence associated mRNAs either enriched in HFD and reduced by ABT-737 treatment, or conversely, reduced by HFD and increased by ABT-737 treatment in mice (*Lmnb1* and *Lbr*). Significance was established using Two-Way ANOVA with multiple comparisons. *, p≤0.05; **, p≤0.01; ***, p≤0.001; ****, p≤0.0001.

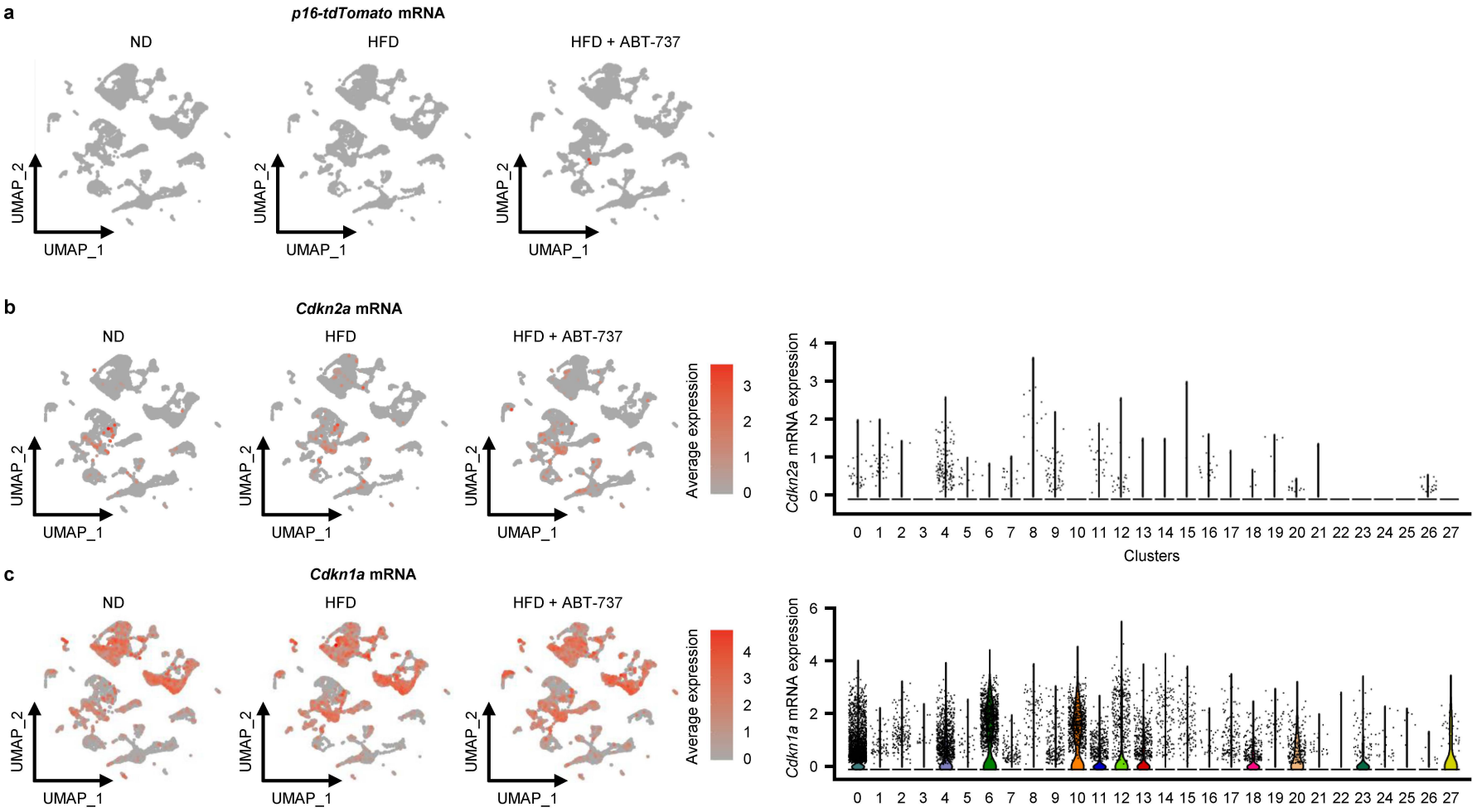

Supplemental Fig. 2 | scRNA-seq analysis of senescence gene expression. a, UMAPs of *p16-tdTomato* mRNA expression in ND, HFD, and HFD + ABT-737 treated mice. **b,** UMAP plot of *Cdkn2a* mRNA expression across all clusters and conditions (*left*). Violin plot of *Cdkn2a* mRNA expression across all clusters (*right*). **c**, UMAP plot of *Cdkn1a* mRNA expression across all clusters and conditions (*left*). Violin plot of *Cdkn1a* mRNA expression across all clusters (*right*). **d,** GSEA SenMayo plots comparing HFD vs ND and HFD + ABT-737 vs HFD for Clusters 15,20, 21, 3, 16, and 27. **e,** GSEA CellAge plots comparing HFD vs ND and HFD + ABT-737 vs HFD for Clusters 6, 17, 7, and 11.

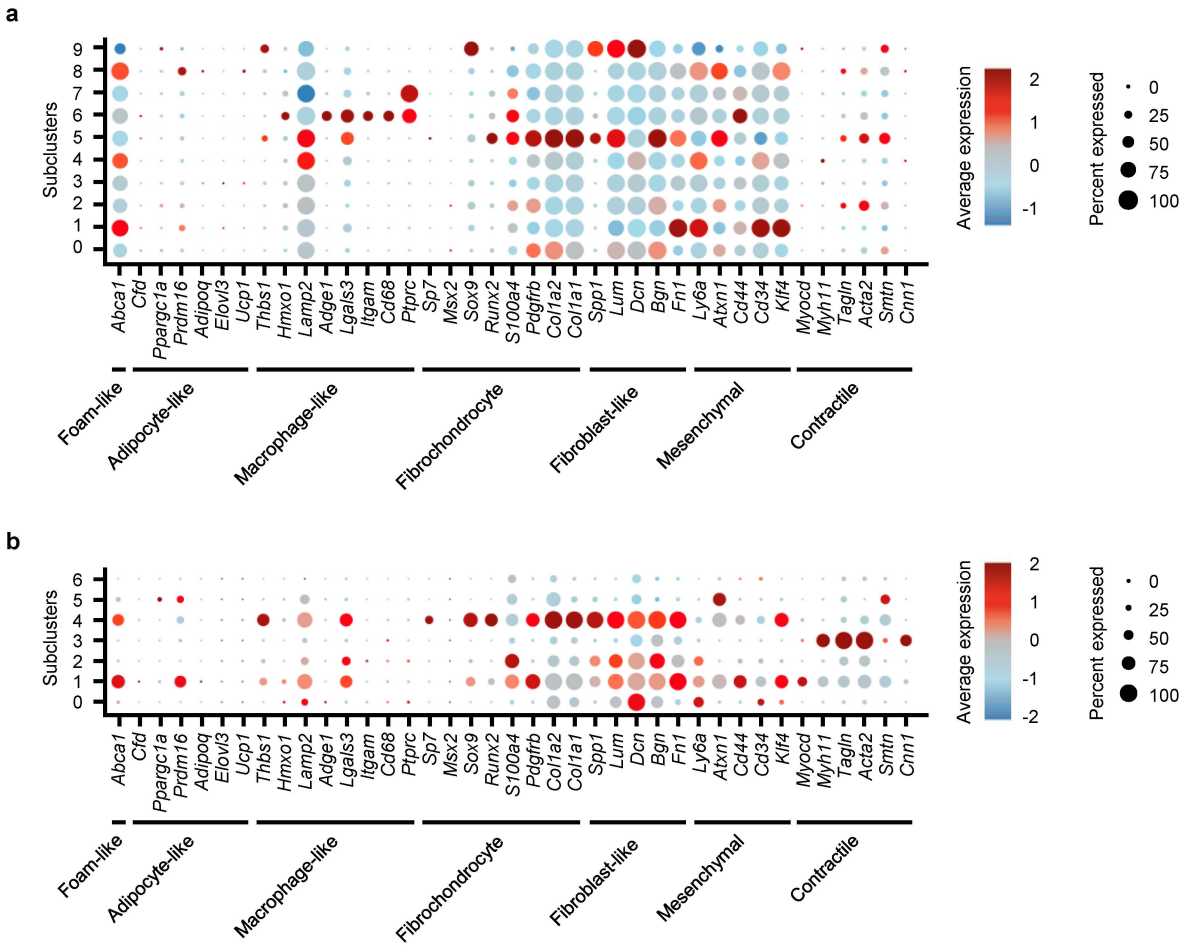

Supplemental Fig. 3 | VSMC phenotype analysis. a, Dot plot representation of the gene expression profile for VSMC phenotype mRNA markers for Cluster 0 subclustered VSMCs. **b,** Dot plot representation of the gene expression profile for VSMC phenotype mRNA markers for Cluster 12 subclustered VSMCs.

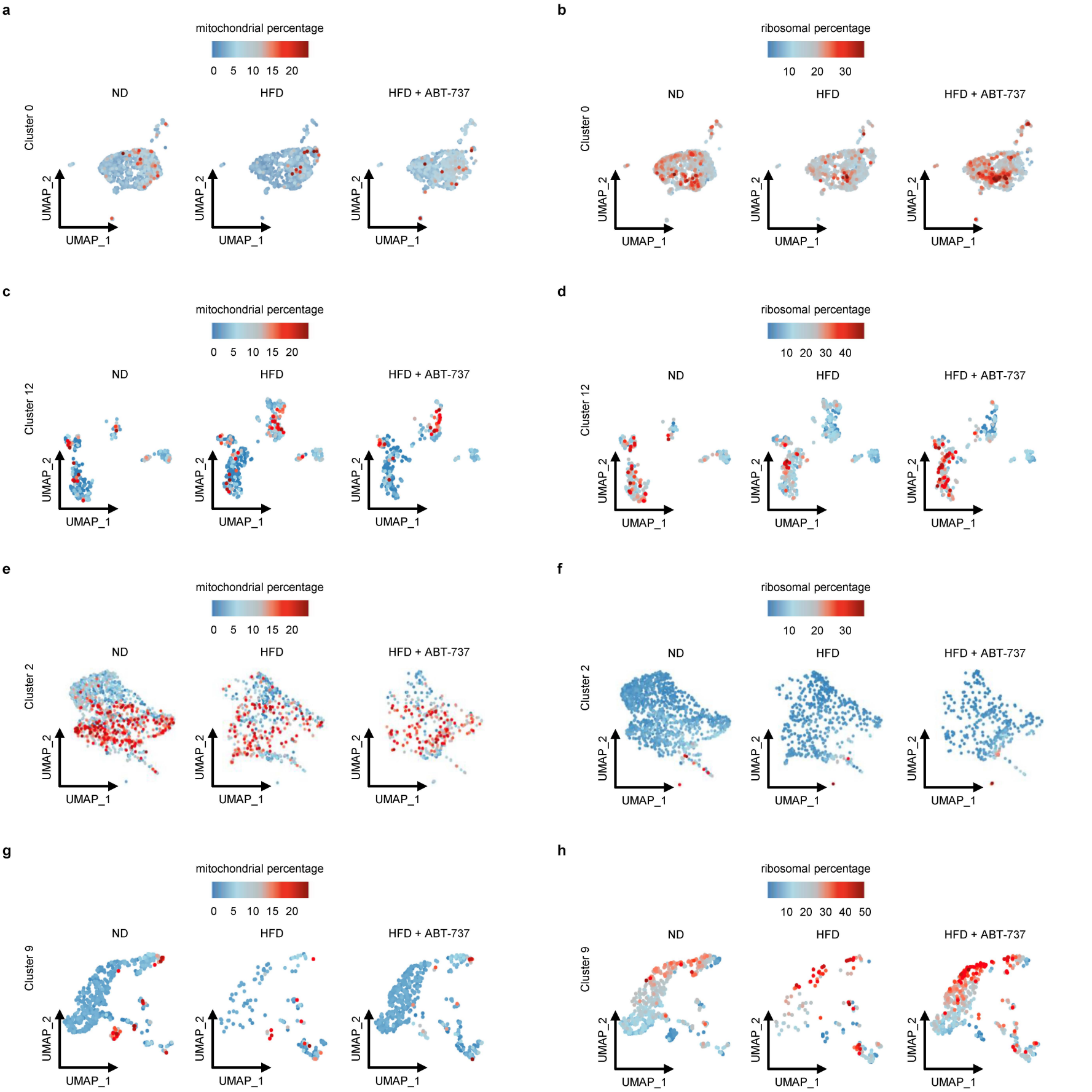

Supplemental Fig. 4 | Analysis of mitochondrial and ribosomal gene expression in cell clusters with senescence features. a, UMAPs of scRNA-seq mitochondrial gene expression across Cluster 0 subclustered VSMCs in ND, HFD, and HFD + ABT-737 treated mice. **b,** UMAPs of scRNA-seq ribosomal gene expression across Cluster 0 subclustered VSMCs in ND, HFD, and HFD + ABT-737 treated mice. **c,** UMAPs of scRNA-seq mitochondrial gene expression across Cluster 12 subclustered VSMCs in ND, HFD, and HFD + ABT-737 treated mice. **d,** UMAPs of scRNA-seq ribosomal gene expression across Cluster 12 subclustered VSMCs in ND, HFD, and HFD + ABT-737 treated mice. **e,** UMAPs of scRNA-seq mitochondrial gene expression across Cluster 2 subclustered fibroblasts in ND, HFD, and HFD + ABT-737 treated mice. **f,** UMAPs of scRNA-seq ribosomal gene expression across Cluster 2 subclustered fibroblasts in ND, HFD, and HFD + ABT-737 treated mice. **g,** UMAPs of scRNA-seq mitochondrial gene expression across Cluster 9 subclustered T-cells in ND, HFD, and HFD + ABT-737 treated mice. **h,** UMAPs of scRNA-seq ribosomal gene expression across Cluster 0 subclustered T-cells in ND, HFD, and HFD + ABT-737 treated mice.

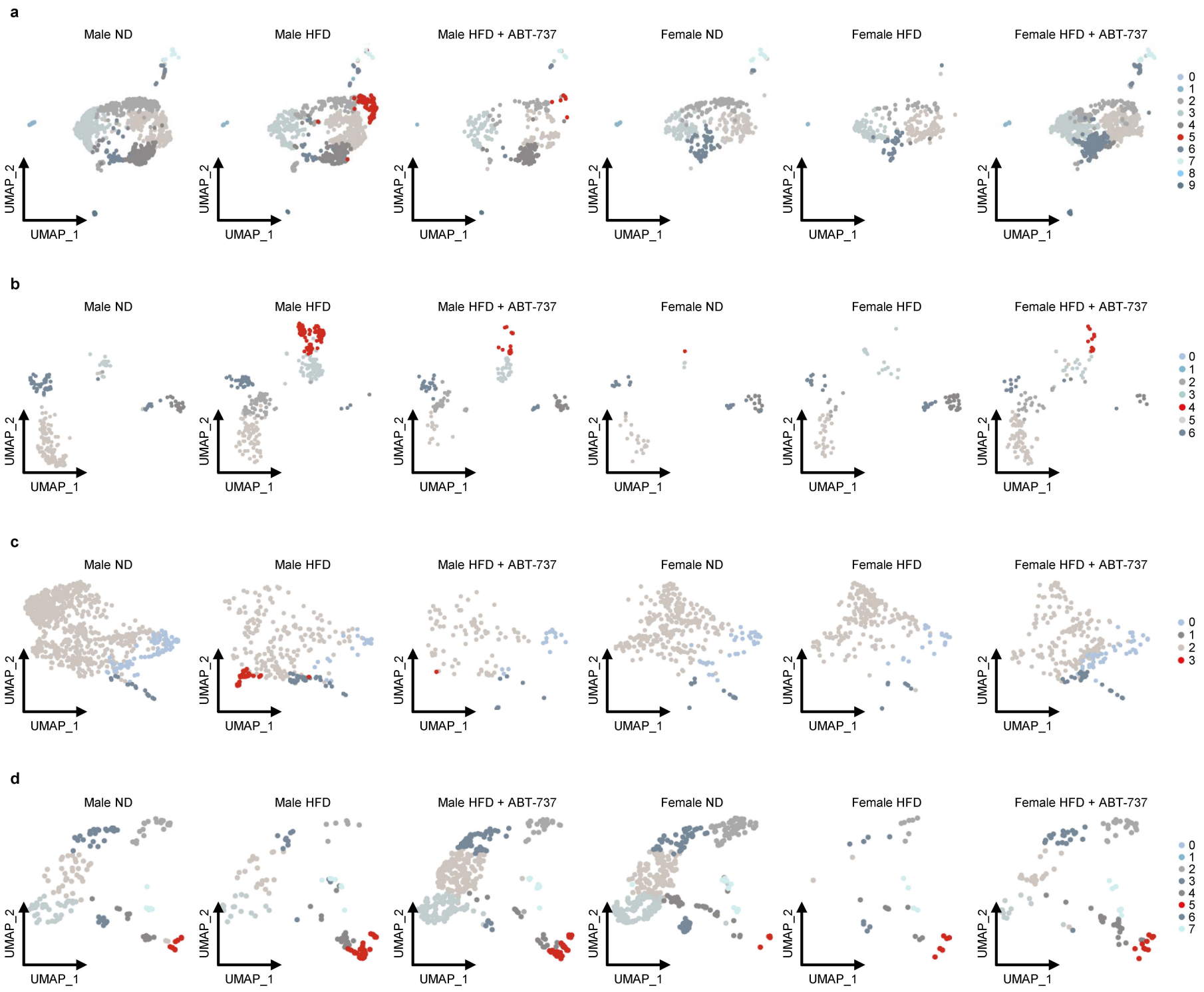

Supplemental Fig. 5 | Sex differences in unbiased subclustering of senescent clusters. a, UMAPs of Cluster 0 subclustering across the ND, HFD, and HFD + ABT-737 groups for male (*left*) and female (*right*) mice. **b**, UMAPs of Cluster 12 subclustering across ND, HFD, and HFD + ABT-737 for male (*left*) and female (*right*) mice. **c**, UMAPs of Cluster 2 subclustering across ND, HFD, and HFD + ABT-737 for male (*left*) and female (*right*) mice. **d**, UMAPs of Cluster 9 subclustering across the ND, HFD, and HFD + ABT-737 groups for male (*left*) and female (*right*) mice.

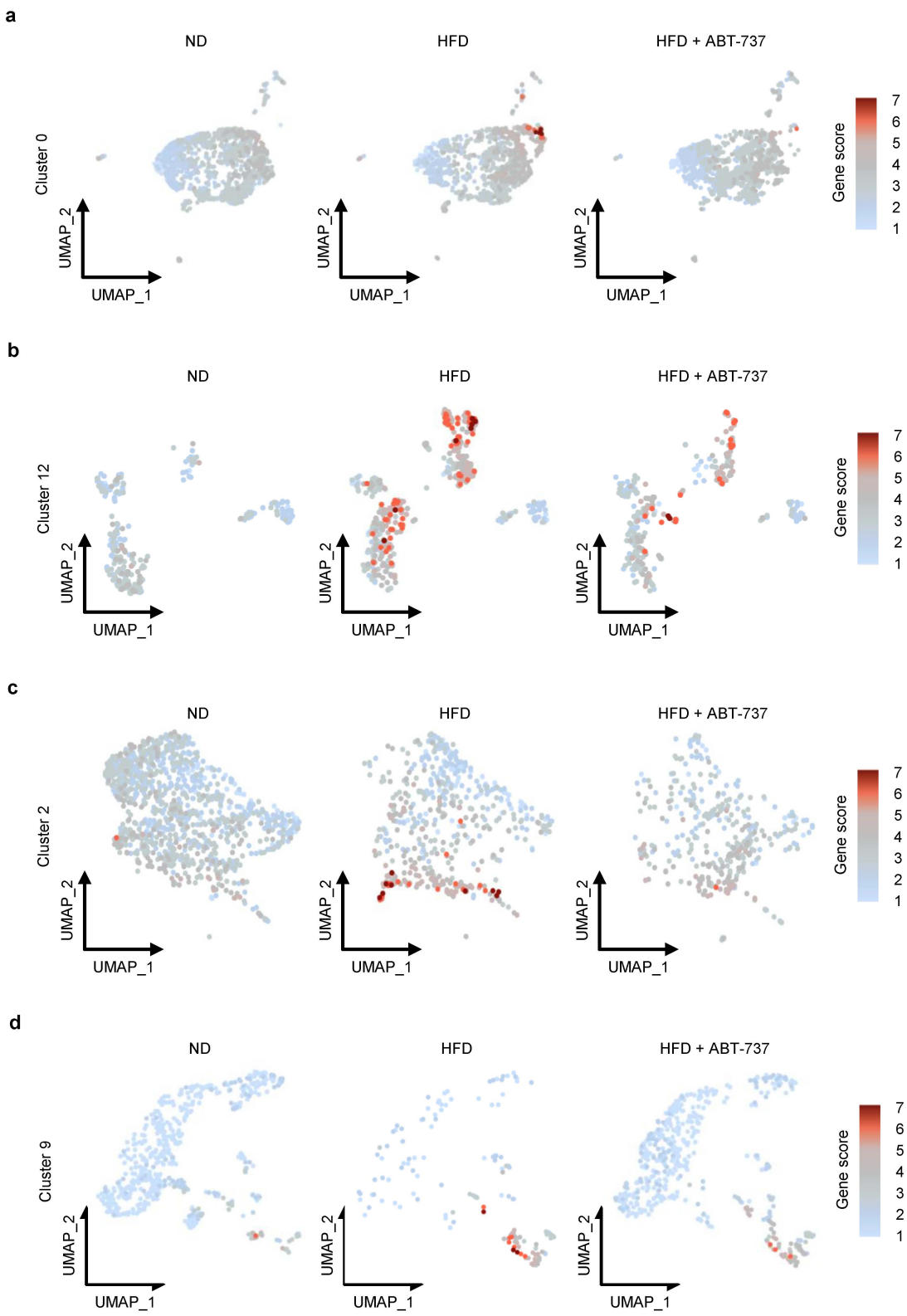

Supplemental Fig. 6 | Vascular senescent score on individual cell clusters. a, UMAPs of vascular-senescence scoring across Cluster 0 VSMCs in ND, HFD, and HFD + ABT-737. **b,** UMAPs of vascular-senescence scoring across Cluster 12 VSMCs in ND, HFD, and HFD + ABT-737. **c,** UMAPs of vascular-senescence scoring across Cluster 2 fibroblasts in ND, HFD, and HFD + ABT-737. **d,** UMAPs of vascular-senescence scoring across Cluster 9 T-cells in ND, HFD, and HFD + ABT-737.

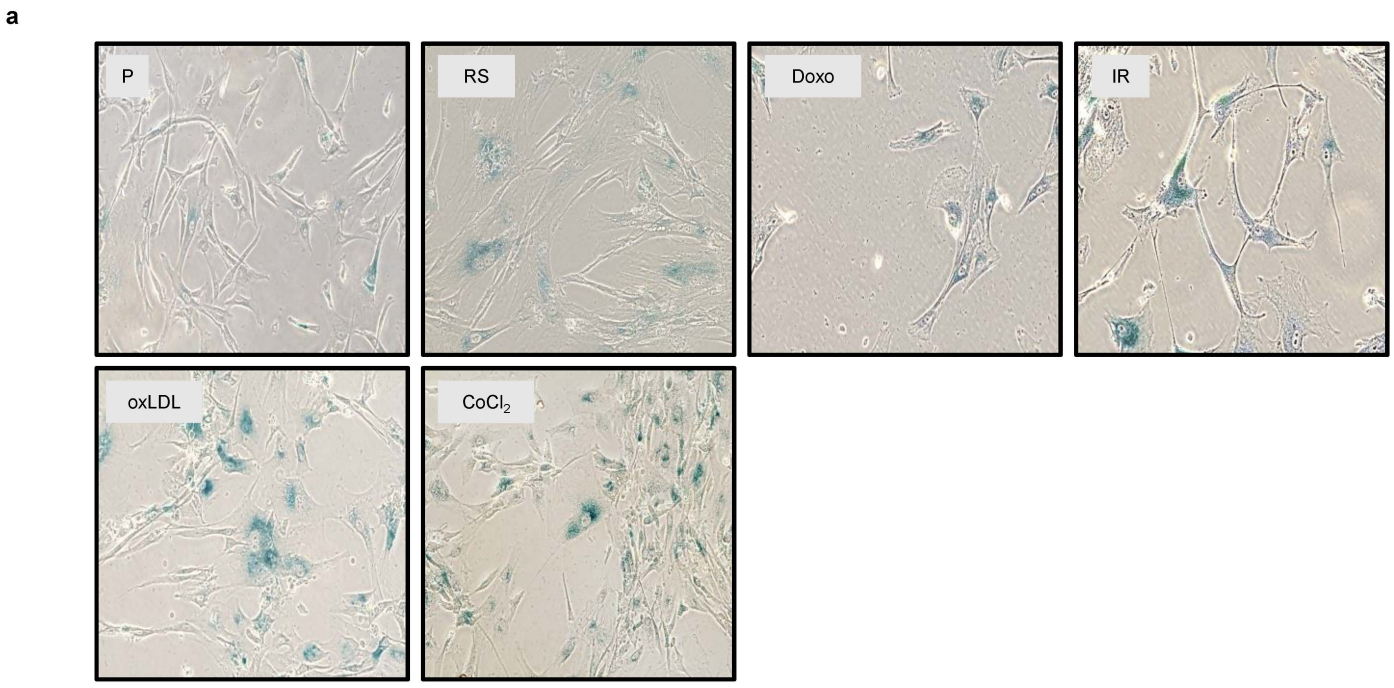

d

Human metadata

Transitional	Fibromyocyte	Fibrochondrocyte	Foam-like	Fibroblast-like
TNFRSF11B	LTBP2	LUM	APOE	LUM
SPAC	MGP	SERPINE2	LUM	CST3
LTBP2	TNFRSF11B	LTBP2	CD9	LGALS3
CD9		CST3	SPARC	
		MGP		

Supplemental Fig. 7 | Human VSMC senescence validation. a, Phase contrast micrographs of SA-βgal activity (blue) staining in proliferating (P), replicative senescence (RS), doxo-treated, IR-treated, oxLDL-treated, and $CoCl_2$-treated human VSMCs for 7-10 days. **b**, RT-qPCR analysis of the levels of *CDKN2A* and *IL8* mRNAs in human VSMCs treated as described in (a). **c**, RT-qPCR analysis of the levels of *MMP3, CTSS*, and *LCP1* mRNAs in human VSMCs treated as described in (a). **d,** Table of human scRNA-seq metadata analysis from atherosclerotic tissue. Each column represents a VSMC phenotype identified in the metadata analysis, and each column includes the vascular senescent scoring genes that were expressed in the indicated VSMC phenotype. In b and c, data represent the means ±SD from n=3 biological replicates. Significance was established using Shapiro-Wilk test first, followed by Welch's t-test. *, p≤0.05; **, p≤0.01; ***, p≤0.001; ****, p≤0.0001.

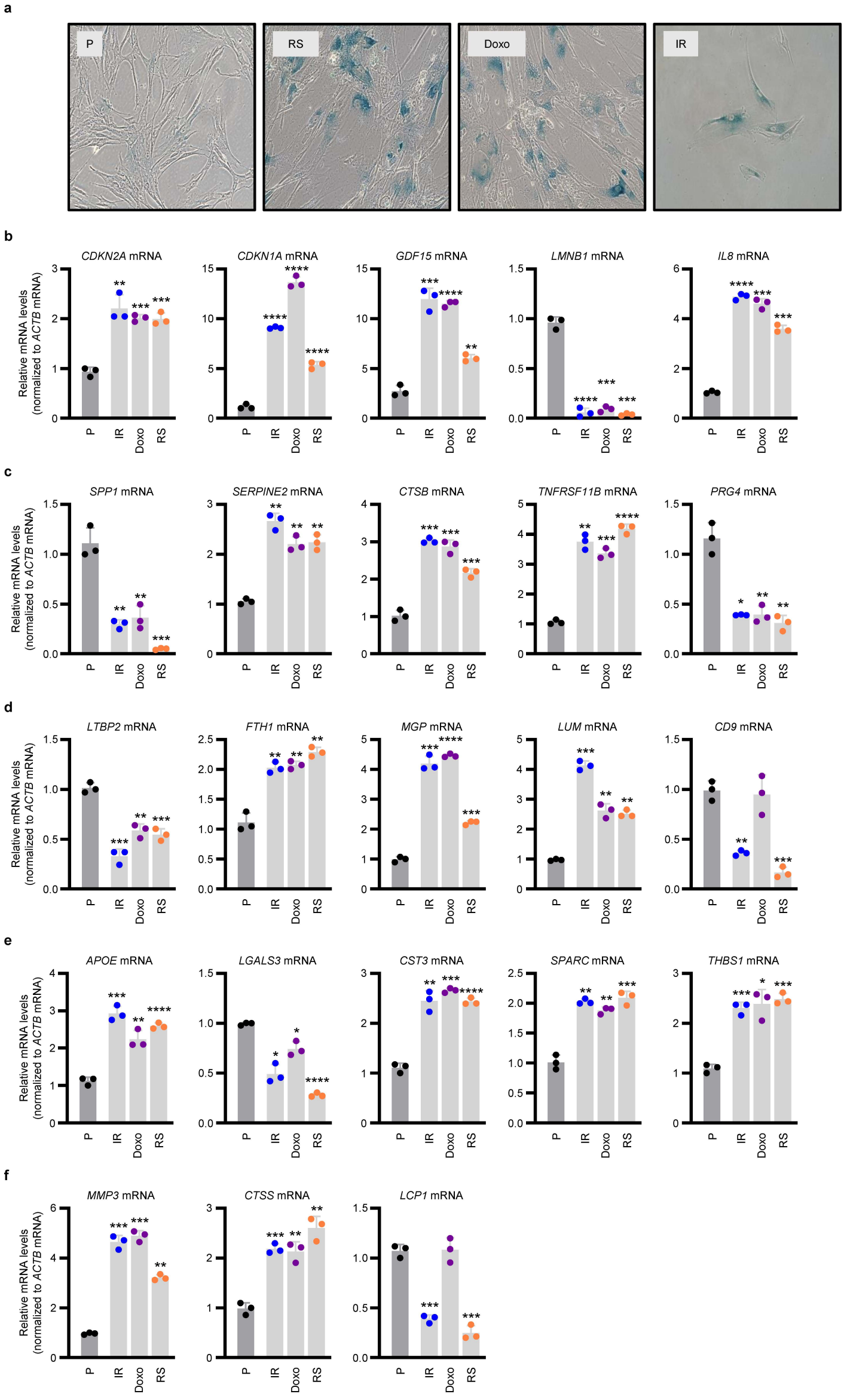

Supplemental Fig. 8 | Human WI-38 fibroblast senescence validation. a, Phase contrast micrographs of SA-βgal activity (blue) staining in human WI-38 fibroblasts that were either proliferating (P), rendered senescent by replicative senescence (RS), or by treatment with Doxo, IR and additional culture for 7-10 days. **b**, RT-qPCR analysis of the levels of *CDKN2A, CDKN1A, GDF15, LMNB1* and *IL8* mRNAs in WI-38 fibroblasts treated as described in (a). **c-f**, RT-qPCR analysis of the levels of *SPP1, SERPINE2, CTSB, TNFRSF11B, PRG4*, *LTPBP2, FTH1, MGP, LUM, CD9, APOE, LGALS3, CST3, SPARC, THBS1*, *MMP3, CTSS, and LCP1* mRNAs in human WI-38 fibroblasts treated as described in (a). In b-f, data represent the means ±SD from n=3 biological replicates. Significance was established using One-Way Anova with multiple comparisons. *, p≤0.05; **, p≤0.01; ***, p≤0.001; ****, p≤0.0001.

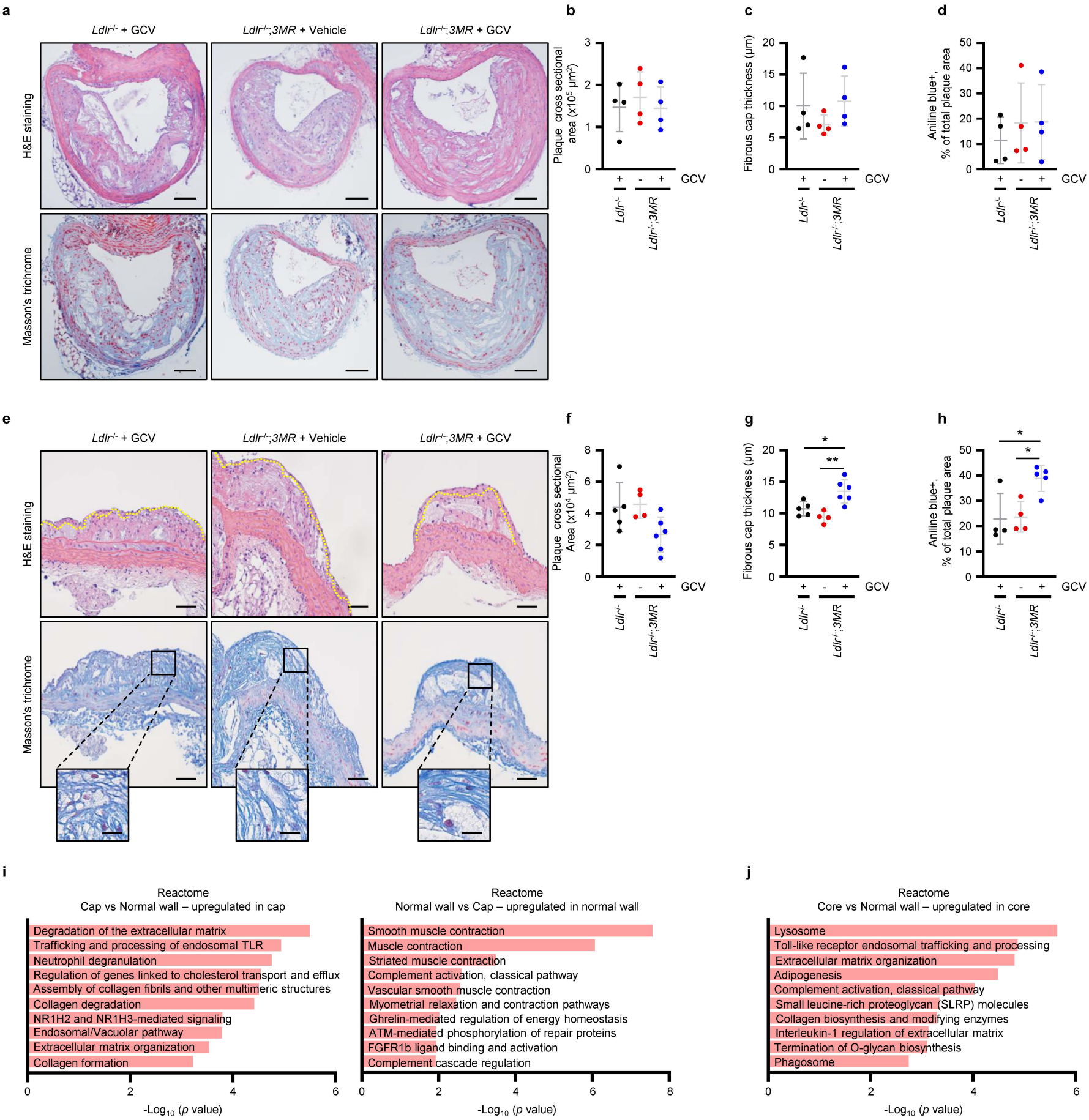

Supplemental Fig. 9 | Analysis for spatial transcriptomic profiling of arterial segments. a, H&E staining (*top*) and Masson's trichrome staining (*bottom*) of brachiocephalic arterial sections from *Ldlr*$^{-/-}$ + GCV, *Ldlr*$^{-/-}$;*3MR* + Vehicle, and *Ldlr*$^{-/-}$;*3MR* + GCV treated mice. The scale bar is 100 µm. **b,** Plaque cross sectional area, **c,** plaque fibrous cap thickness measurements and **d,** Masson's trichrome analysis of Aniline blue-positive area over total plaque area in brachiocephalic arterial sections from *Ldlr*$^{-/-}$ + GCV, *Ldlr*$^{-/-}$;*3MR* + Vehicle, and *Ldlr*$^{-/-}$;*3MR* + GCV treated mice. **e,** H&E staining (*top*) and Masson's trichrome staining (*bottom*) of the descending aortic sections from *Ldlr*$^{-/-}$ + GCV, *Ldlr*$^{-/-}$;*3MR* + Vehicle, and *Ldlr*$^{-/-}$;*3MR* + GCV treated mice. The scale bar is 50 µm. **f,** Plaque cross sectional area, **g,** plaque fibrous cap thickness measurements (cap is underlined with yellow dashed line), and **h,** Masson's trichrome analysis of Aniline blue-positive area over total plaque area in sections of the descending aorta from *Ldlr*$^{-/-}$ + GCV, *Ldlr*$^{-/-}$;*3MR* + Vehicle, and *Ldlr*$^{-/-}$;*3MR* + GCV treated mice. Inset image scale bar is 5 µm. **i,** Reactome pathway analysis of genes upregulated in cap compared to normal wall across all conditions (*left*) and of genes upregulated in the normal wall compared to the cap (*right*). **j**, Reactome pathway analysis of genes upregulated in the core compared to the normal wall across all conditions. Significance was established using One-Way Anova with multiple comparisons. *, p≤0.05; **, p≤0.01; ***, p≤0.001; ****, p≤0.0001.